Available online at www.sciencedirect.com
ScienceDirect
International Journal of Multiphase Flow 33 (2007) 498–509
International Journal of Multiphase Flow
www.elsevier.com/locate/ijmulflow

Three-phase upward flow in a vertical pipe

Fadel F. Erian [a,*,1], Leonard F. Pease III [b,2]

[a] IF&G Inc., Materials Handling Division, P.O. Box 985, Richland, WA 99352, United States
[b] Department of Chemical Engineering, Princeton University, Princeton, NJ 08544, United States

Received 3 August 2006; received in revised form 19 December 2006

Abstract

In this paper we develop an approach to design a three-phase, gas–solid–liquid flow system that transports pneumatically scarified solid particles, including sticky ones, through a vertical pipe. The proposed system permits the introduction and maintenance of a liquid film that coats the pipe's inner wall and acts as a lubricant that ensures sticky particles continue to move upward without permanently adhering to the pipe wall. The system's operating conditions fall within the boundaries of the annular dispersed region on a typical flow pattern map of vertical flow of a gas–liquid mixture. High gas superficial velocities combined with low liquid superficial velocities characterize such a region. A combination of a modified one-dimensional, two-fluid annular dispersed flow model and a one-dimensional pneumatic conveying model is shown to describe this transport process satisfactorily. Solution of the combined models produces all the necessary design parameters including power requirements and superficial velocities of the two-fluid media needed to transport a given amount of solid particles. Results of model calculations are compared with rare three-phase flow data obtained prior to the development of the present model, by an independent experimental team that used the physical conditions of the present approach. Reasonable agreement justifies the use of the combined model for engineering design purposes.
Published by Elsevier Ltd.

Keywords: Three-phase flow; Annular dispersed flow; Pneumatic conveying; Pressure drop in vertical pipe

1. Introduction

Millions of gallons of toxic and radioactive waste are being stored in large underground tanks at several Department of Energy sites. At the Hanford Site 37 million gallons of such waste are stored in 149 aging underground single shell tanks located approximately 20 miles from the Columbia River Basin. The waste composition in each tank varies, but usually includes a combination of liquids, gas-trapping sticky sludge and hard, rock-like salt cake. Many of these tanks leak, requiring the contained waste to be transferred to safer storage or pretreatment facilities. Many specialized technologies need to be developed to deal with

* Corresponding author. Tel.: +1 509 585 9484; fax: +1 509 585 0471.
E-mail address: faferian@msn.com (F.F. Erian).
[1] Staff Scientist, Battelle, Pacific Northwest National Laboratory, Richland, WA, United States, during the conduct of this work.
[2] Present address: NIST, 100 Bureau Drive, Mail Stop 8362, Gaithersburg, MD 20899-8362, United States.

0301-9322/$ - see front matter Published by Elsevier Ltd.
doi:10.1016/j.ijmultiphaseflow.2006.12.007

the mobilization, retrieval, transport and reliable delivery of large amounts of toxic and radioactive waste to such facilities.

A class of storage tanks can utilize pneumatic conveying for the retrieval of scarified solids, occasionally laced with sticky sludge. One approach to removing the waste incorporates a mechanically articulated arm deployed through a center opening at the top of a tank and is able to position a special "end effector" to virtually any location within the interior of the tank to treat and/or remove the waste. One such end effector is capable of pulverizing a salt cake layer floating over a pool of very viscous and sticky liquid, using very high-pressure water jets. The pulverized solids are then conveyed pneumatically upward to ground level. After the solid particles are removed from the tank they are mixed with appropriate liquids to form slurries that are transported through a pipeline to new storage or pretreatment facilities. The formation of a thin liquid film that travels upwards along the inner wall of a vertical retrieval pipe is thought to prevent those particles laced with the sticky sludge from adhering to the wall and eventually causing instability and blockage.

In this paper we describe a new approach to calculate the pressure drop in a flowing three-phase mixture. The approach enables design of a system for reliable transport of the pulverized solid material from the interior of a typical underground storage tank.

2. Background

Pneumatic conveying is a potentially effective technology for the retrieval of pulverized solids from underground storage tanks. It is very likely that these solids, frequently surrounded by very viscous and sticky liquids will be laced with such liquids. Tests on sticky solids simulants show that during vertical pneumatic transport, solid particles thrown against the wall due to the turbulence in the conveying air tend to stick to it. These particles accumulate to form thick barriers that lead to unstable conveyance and eventual blockage of the pipe. In this work we propose to inject a lubricating liquid film into the pneumatic conveying pipe that forms a stable film at the pipe wall under specific two-phase flow conditions. We extend a model of the annular dispersed two-phase gas–liquid flow regime to include transport of solid particles within its fast moving core region. Thus, we propose a specially tailored three-phase flow system capable of transporting sticky solids pneumatically.

3. Model development

The model presented here integrates two sub-models to produce a design method for three-phase gas–solid–liquid upward flow in a circular pipe. Experimental data obtained earlier with air, water and a variety of sand particles provides a convenient test case for the model given the scarcity of three-phase flow data in the literature (Liljegren et al., 1995). The present model calculations may be considered as one method to analyze such data.

The first sub-model is a modified version of Oliemans, Pots and Trompé's model, (1986), (referred to subsequently as the OPT model), for annular dispersed gas–liquid flow in vertical pipes (Fig. 1b). The second sub-model is a phenomenological, one-dimensional model for upward gas–solid flow in vertical pipes that is essentially a pneumatic conveying model (Fig. 1c). The following sections present a summary of these two sub-models followed by their integration into the present model (Fig. 1d).

3.1. Modified OPT model

When gas and liquid flow together in a pipe, a variety of flow patterns emerge. These have simple or complex gas–liquid interfaces, ranging from distributed bubbles or droplets to more distinctive and geometrically complex interfaces. Fig. 1b illustrates the geometry of annular dispersed upward flow in a vertical tube. The OPT model employs this flow pattern in its development. We include here the main equations that describe the physical features of this flow in preparation for solving the modified OPT model and subsequently the integrated model. We refer the reader to Oliemans et al. (1986) to obtain additional formulae and details.

In annular dispersed flow, the liquid is distributed axisymmetrically within a relatively thin film at the pipe wall, with some droplets entrained in the gas stream within the core of the pipe. The liquid at the wall is

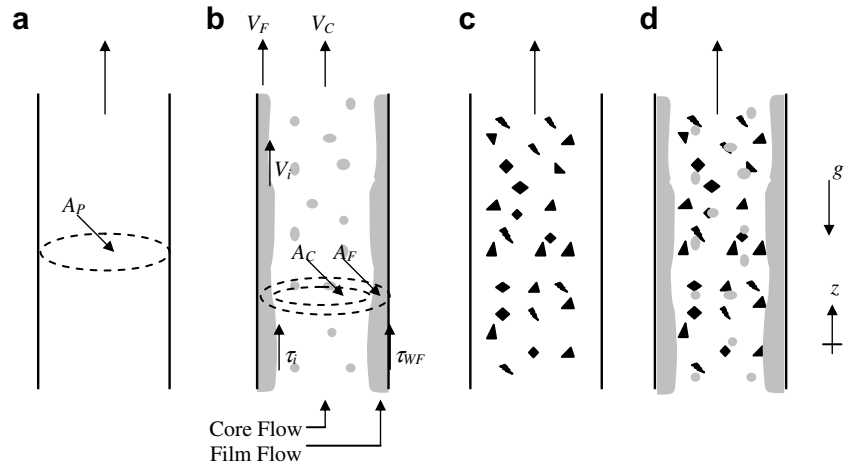

Fig. 1. Schematic diagram of the various flow phases representing the integrated model components. Size of solid particles (black) and liquid droplets (gray) are exaggerated for clarity. (a) Gas flow, (b) gas–liquid annular flow, (c) gas–solid flow and (d) gas–liquid–solid flow.

regarded as one phase and the gas plus entrained droplets in the core as the second. The following assumptions are made:

- The flow is a one-dimensional, concurrent, upward, steady, and fully developed two-phase flow with negligible heat or mass transfer between phases.
- The liquid and gas have constant physical properties.
- The liquid and gas mass flow rates, W_L and W_G, their values per unit pipe cross-sectional area, G_L and G_G, or their superficial velocities, V_{SL} and V_{SG}, are given.
- The liquid droplets in the core are small and travel at the gas speed, i.e., without slip.
- The liquid film is thin relative to the pipe radius, the flow within it is fully turbulent and the film surface is wavy.

The assumption of constant and steady two-phase flow parameters is not very restrictive. Steadiness implies that entrained liquid droplets deposit on the film surface at the same rate that new droplets are sheared off the film's wavy surface. In other words, the net amounts of liquid in both the film and the core do not vary significantly with time or vertical position, which is a reasonable assumption over a short length of pipe. For longer lengths where these parameters might vary due to changes in the physical properties of the phases, results can be obtained by incremental integration.

Applying momentum balances to the pipe core and the total pipe contents yield

$$-\frac{\partial p}{\partial z} = \rho_C g + \frac{\tau_i P_i}{A_C} \tag{1}$$

and

$$-\frac{\partial p}{\partial z} = (\alpha_F \rho_L + \alpha_C \rho_C) g + \frac{\tau_{WF} P_F}{A} \tag{2}$$

with

$$\alpha_F + \alpha_C = 1, \tag{3}$$

where

$\partial p/\partial z$ pressure drop per unit length along the axial direction, $+z$
ρ_C, ρ_L core and liquid mass densities
τ_i, τ_{WF} interfacial and wall shear stresses

P_i, P_F interface and wall perimeters, πD_C and πD, respectively
A_F, A_C cross-sectional areas occupied by film and core, respectively
D_F, D_C hydraulic diameters of the film and the core, $\alpha_F D$ and $\sqrt{\alpha_C} D$, respectively
α_F, α_C film and core hold-ups defined as A_F/A and A_C/A, respectively
V_F, V_C average film and core velocities defined as V_{SF}/α_F, and V_{SC}/α_C, respectively
A pipe cross-sectional area, $\pi D^2/4$
V_{SF} $(G_L - G_{LE})/\rho_L$, the superficial velocity of the film
V_{SC} $(G_G + G_{LE})/\rho_C$, the superficial velocity of the core
V_{SG} G_G/ρ_G, the superficial velocity of the gas
G_{LE}, G_C superficial entrained liquid mass flux and core, respectively
Re_C $G_C D_C/\mu_C$, the Reynolds number of the core
Re_F $\rho_L V_F D_F/\mu_L$, the Reynolds number of the film
D pipe diameter
g gravitational constant

The core mass density, ρ_C, is determined from volume-averaging over the core, and, the core viscosity, μ_C, is defined using the mixing rule as in Oliemans et al. (1986). The film hold-up, α_F, is related to the film thickness, h_F, as follows:

$$\alpha_F = 4\frac{h_F}{D}\left(1 - \frac{h_F}{D}\right). \tag{4}$$

The total liquid hold-up, α_L, follows from adding the volume fraction of liquid entrained to the film hold-up:

$$\alpha_L = \alpha_F + (1 - \alpha_F)\frac{V_{SLE}}{V_{SLE} + V_{SG}}, \tag{5}$$

where V_{SLE} is the superficial velocity of entrained liquid.

Eliminating the pressure drop by combining Eqs. (1) and (2) leads to a relationship from which the film hold-up can be determined:

$$\frac{\tau_{WF} P_F}{A} - \frac{\tau_i P_i}{A_C} + \alpha_F \Delta\rho g = 0, \tag{6}$$

where

$$\Delta\rho = \rho_L - \rho_C. \tag{7}$$

The shear stresses τ_i and τ_{WF}, in Eq. (6), are calculated from:

$$\tau_i = \frac{1}{2} f_i \rho_C (V_C - V_i)|V_C - V_i|, \tag{8}$$

$$\tau_{WF} = \frac{1}{2} f_F \rho_L V_F^2. \tag{9}$$

Using the previously defined Reynolds numbers, $f_i = f_i(Re_C, \varepsilon_i/D_C)$ and $f_F = f_F(Re_F, \varepsilon/D)$ are Fanning friction factors obtained using the explicit formulae of Serghides (1984), and ε_i and ε are the relative interface and wall roughness, respectively. The equations summarized herein form a closed set, provided relations are available for the Fanning friction factors, f_i and f_F, the interface velocity, V_i, the interface roughness, ε_i, and the entrained liquid fraction, E, which is defined as

$$E = \frac{W_{LE}}{W_L}. \tag{10}$$

We also define the relative entrainment such that

$$\frac{E}{1 - E} = \frac{W_{LE}}{W_{LF}},$$

where

W_{LE} entrained liquid flow in the core
W_L total liquid flow
W_{LF} liquid flow in the film

We employ here the expressions reported in Oliemans et al. (1986) for the first four variables, f_i, f_F, V_i and ε_i, but use a different empirical model to calculate the entrained liquid fraction, E, and the associated relative entrainment term. This is the main modification to the OPT model as applied here.

Nearly 800 data points reported in eighteen references that are listed in Oliemans et al. (1986), represent most of the available measurements of annular dispersed flow in vertical tubes. References identifying these published papers and reports are not included here for brevity. One of the measured quantities is the entrained liquid fraction, E. Multiple linear regression was applied to this data using a large number of dimensionless groups thought to influence, directly or indirectly, the entrainment phenomenon in vertical upward annular dispersed flow. The following empirical formula for the relative entrainment resulted from the statistical analysis:

$$\frac{E}{1-E} = 29.2(Ku)^{-1.60}(Fr_L)^{+0.52}(We)^{-0.20}(\mathrm{DR}_g)^{+0.65}(\mathrm{VDR}_L)^{-0.08} \tag{11}$$

where

Ku Kutateladze number, $\rho_G^{0.5} V_{SG}/(\Delta\rho' g\sigma)^{0.25}$
Fr_L Froude number for the liquid phase, V_{SL}^2/gD
We Weber number for the liquid phase, $\rho_L V_{SL}^2 D/\sigma$
DR_g gas densimetric ratio, $\rho_G/\Delta\rho'$
VDR_L liquid visco-densimetric ratio, $(\mu_L\rho_L)/(\mu_G\Delta\rho')$

with

$$\Delta\rho' = \rho_L - \rho_G, \tag{12}$$

ρ_G density of the gas
σ liquid surface tension coefficient

Given a set of superficial velocities for the liquid and gas, their physical properties and a pipe diameter, Eq. (6) can be solved numerically by assuming an initial value for α_F. Numerical iterations start with a reasonably large value for this parameter. It is then incrementally reduced until the correct value of α_F is reached when Eq. (6) is satisfied. Values of the left hand side of Eq. (6), as a function of α_F for two sample cases are shown in Fig. 2. In Fig. 2a, physical conditions result in a solution with two roots, a trivial root, $\alpha_F \cong 0$, and, a second root, $\alpha_F = 1$, that corresponds to a single-phase liquid flow. Flow conditions for Fig. 2b produce three roots. The largest of the three corresponds to a film thickness approaching the pipe radius, and thus to flow conditions far removed from those of annular dispersed flow according to Taitel et al. (1980). The smallest root corresponds again to $\alpha_F \cong 0$ and produces a very thin film that is physically impractical to maintain due to surface tension and evaporative effects. Oliemans et al. (1986) excluded the smallest and largest roots and selected the middle root as we do here. A formal stability analysis by Barnea and Taitel (1992, 1994), show the middle root to be the only valid stable root. The proper solution to Eq. (6) gives the correct value of α_F and, consequently, most of the other parameters that depend on it. Finally Eq. (2) yields the pressure drop for the given set of superficial velocities.

3.2. The pneumatic conveying model

This section describes an approach to design a system to transport dry coarse solid particles upward in a vertical pipe. It utilizes a phenomenological, bulk effect model based on physical descriptions of the mechanisms involved in the transport process, as in Govier and Aziz (1972). Pipes used in this pneumatic conveying application may have inside diameters between 0.05 and 0.15 m. Particles may have a variety of geometrical shapes with effective mean diameters d_m, which vary between $500 \leqslant d_m \leqslant 5000$ μm, as shown in Table 1. The

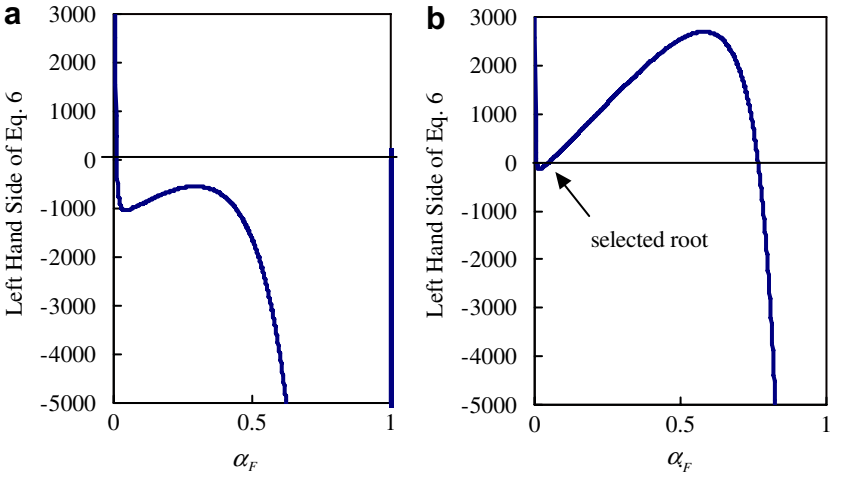

Fig. 2. Typical solutions to Eq. (6) showing (a) a single root solution and (b) a three root solution.

effective mean diameter of the particles should not exceed the turbulence integral scale that is on the order of one tenth of the pipe radius, in order to avoid possible laminarization.

For a specific application, the solid particles are assumed to have one shape type, such as angular with flat surfaces, curved with smooth surface, etc., and a narrow particle size distribution with a unique mean diameter, d_m. These particle characteristics determine the value of the empirical parameter (f_S/f_G) in Eq. (13). Fig. 1c depicts the geometry of upward pneumatic conveying through a vertical pipe as employed here.

We consider here a phenomenological model that describes the upward, steady state transport of solid particles in air. It permits the calculation of the overall pressure drop through a straight vertical pipe section. The pipe conveys a dilute phase dry air–solid mixture between two prescribed points along the positive z-direction, as shown in Fig. 1c. In the dilute phase regime, particle–particle interactions are negligible during transport. The physical properties of both the conveying air and the solid particles as well as their shape, settling velocities and material properties are known. The pressure drop per unit length of that pipe is obtained by integrating the following first order differential equation along its length

$$\underset{\text{I}}{\frac{\mathrm{d}p}{\mathrm{d}z}} = \underset{\text{I}}{-\frac{1}{2}\left(\frac{f_G}{D}\right)\rho_G V_{SG}^2} \underset{\text{II}}{-\frac{1}{2}\left(\frac{f_G}{D}\right)\left(\frac{f_S}{f_G}\right)\rho_S V_{SS}^2} \underset{\text{III}}{-\rho_S g}, \tag{13}$$

where the three terms represent,

I pressure drop per unit length due to air–wall friction
II pressure drop per unit length due to the solids effect on air–wall friction
III pressure drop per unit length due to elevation change of the solids load

The pressure drop due to the solids-wall friction is assumed negligible since the solids contact with the wall is only due to the lateral component of the turbulent velocity without the assistance of gravity. In the above equation

Table 1
Physical properties of the solid particles

Particle type	Particle diameter (μm)	Solids density (kg/m^3)	Bulk density (kg/m^3)	Shape
Small	610	2730	1680	Irregular
Medium	1700	2730	1631	Irregular
Large	4800	2730	1490	Irregular

p	local pressure
z	vertical coordinate direction, upward is positive
D	pipe inside diameter
f_G, f_S	friction factors for the gas and solids, respectively
ρ_G	gas density
V_{SG}	superficial gas velocity
V_{SS}	solids slip velocity, $= V_{SG} - V_T$
V_T	terminal velocity of the solid particles in the transporting gas
f_S/f_G	a friction factor ratio describing the influence of the solids on the air friction, $0 \leqslant f_S/f_G \leqslant 1.0$

A large number of data points were collected in the air–gas flow configuration, depicted in Fig. 1c, that allowed the determination of the empirical friction factor ratio (f_S/f_G), for each of the two pipe sizes used in the experimental program. The pressure drop due to elevation is calculated according to the inventory of solids inside the pipe. Eq. (13) is solved numerically using a 4th order Runga–Kutta approximation.

3.3. The integrated model

The overall pressure drop due to the upward three-phase flow of a gas–solid–liquid mixture in a vertical pipe, as depicted in Fig. 1d, is calculated by simple superposition. A block diagram, Fig. 3, shows the solution strategy followed herein. Only when the flow conditions show the gas–liquid system to be in the annular dispersed flow regime on a two-phase flow pattern map, does the modified OPT model determine the pressure drop. The pneumatic conveying model calculates the pressure drop of the gas–solid mixture when flowing in a similar pipe, at the same gas flow rate and a given solids loading. The overall pressure drop is the sum of these two components less the pressure drop due to the air alone since it is accounted for twice – once in each flow configuration. The integrated model calculations are compared with experimental data in a latter section.

4. The experiment

The experimental data used in this work was obtained over three years prior to the beginning of this work and by a different research team. One of the motivations for this modeling effort was to provide a rigorous

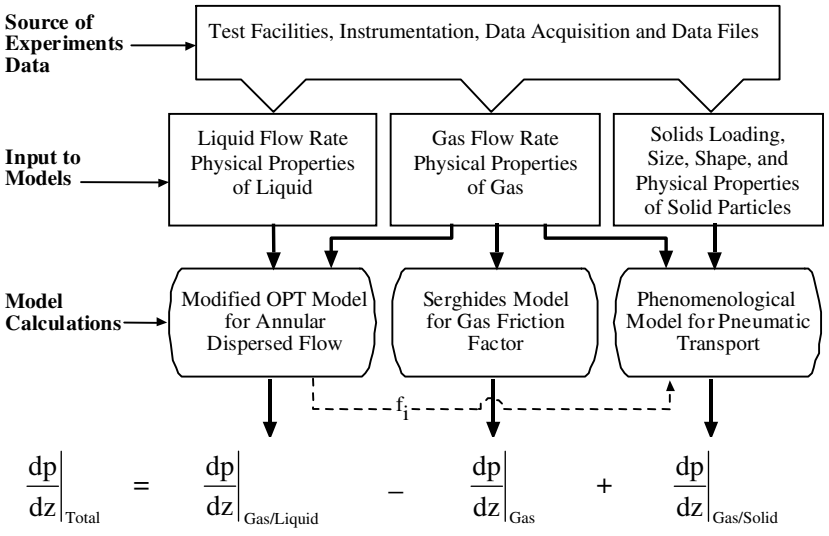

Fig. 3. Solution strategy for the integrated model to determine the total pressure drop for this three-phase flow.

approach to interpret the experimental data, and to guide future plans to conduct additional experiments on the same subject. No formal report was issued that contain tabulated raw data, but we are grateful to the original experimental team for allowing us complete access to the data acquisition files from which we extracted the raw data. Three-phase upward flow experiments of air, sand and water were performed in two separate test facilities that are very similar to the schematic diagram shown in Fig. 4. One had a 5 m high, 10 cm diameter test section, and the other had a 6 m high, 5 cm diameter test section. Guidance was provided to the research team at the start of their experimental program as to the ranges of air and water superficial velocities that would produce annular dispersed upward flow in both vertical pipes in order to include them into their test conditions.

4.1. Experimental facilities, instrumentation and data acquisition

Two separate test facilities were used to obtain the three-phase flow data, one with a 5 m high, 10 cm diameter test section and the other with about 6 m high, 5 cm diameter test section. Sufficiently long transition pipe lengths preceded both test sections to ensure fully developed flow with the solid particles being fully accelerated when they entered the test sections. Suction from powerful blowers induced flow into the test sections. The air flow rate was controlled and adjusted using a bleed valve located prior to the blower intake, a spray ring near the entrance to the transition section introduced water into the system, and a solid particle feeder mounted on precise load cells introduced measured amounts of solid particles into the pipe through a rotary valve and prior to the water spray ring, as shown in Fig. 4. An air–solid/liquid separator allowed only the air to continue into the blower.

Pressure drop measurements were obtained simultaneously from outputs of both absolute pressure transducers (AP), and differential pressure transducers (DP), local temperatures from thermocouples, solids mass flow rate from indications of the solids feeder weight change, water flow rate from a flow meter, and a

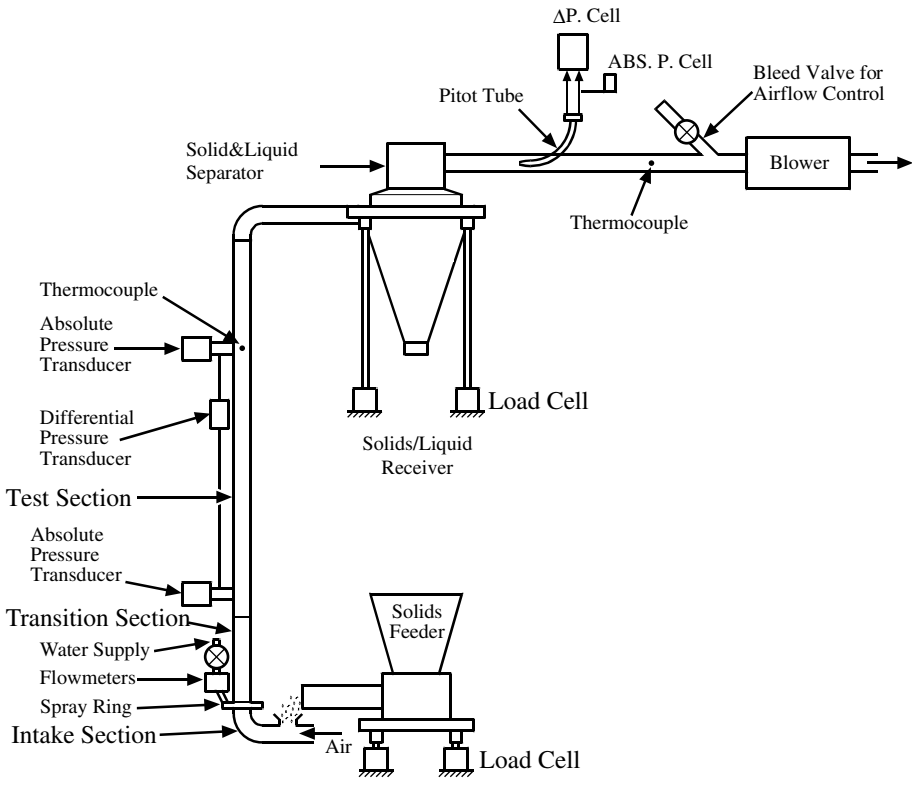

Fig. 4. Arrangement of the experimental facilities showing major components and the measurement systems.

calibrated Pitot Static tube positioned downstream of the air–solid/liquid separator was used to determine the overall air flow through the system. Data were collected digitally using a specially designed data acquisition system and recorded in special files that identified the test run number, and the materials transported through the system.

4.2. Experimental data

Fig. 5 shows data points extracted from a typical data file that was created during a typical test run. Each point represents an average pressure drop value obtained from a recorded time series at the flow conditions of the test run. A typical test sequence begins by allowing air alone to flow through the pipe. When the flow has stabilized at the desired air flow rate, comparison is made between the measured pressure drop as obtained from the instrumentation and a calculated value determined from an appropriate friction factor formulae for this single phase air flow. This procedure was repeated at the beginning of each test run as a calibration process to ensure the reliability and accuracy of the instrumentation system and to confirm proper operation of the equipment. Next, liquid is injected through the spray ring at the desired rate, and after the instruments outputs have stabilized, data were collected for the air–liquid flow situation. However, no attempt was made during these tests to visually observe the occurring flow pattern for this two-phase flow situation and, therefore, was not reported. After a sufficient time record was collected during the gas–liquid flow, solids were fed into the stream in a steady measured rate and pressure drop data recorded after the flow has again stabilized. Progressively increasing and then decreasing the solids loading produced data for several solids transport conditions associated with a given set of gas and liquid flow rates as shown in the figure.

All data points shown here are group averages of sampled data in a recorded time series. Each data point had to pass several acceptance criteria including confidence in the proper functioning of the instrumentation and the data acquisition system, in addition to our own criteria concerning the prevailing flow pattern. Only those data points falling within the annular dispersed flow regime according to the flow pattern map of Taitel et al. (1980) received subsequent analysis. The two vertical lines shown in Fig. 6, one for each pipe diameter, represent the transition boundary between intermittent/slug and annular dispersed upward flows through vertical pipes. The figure also shows the ranges of the air and water superficial velocities used during tests

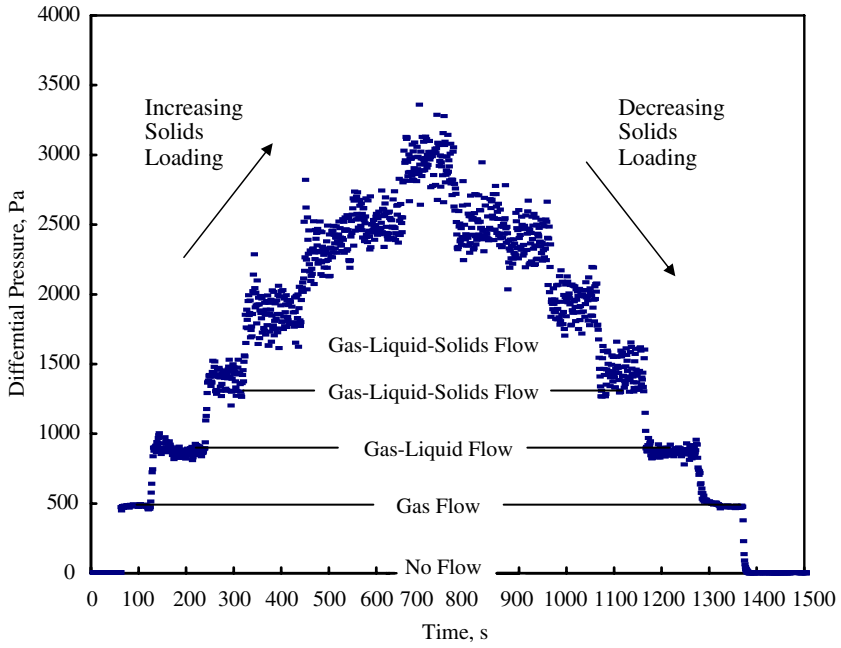

Fig. 5. Pressure drop data versus time collected during a typical three-phase flow test run.

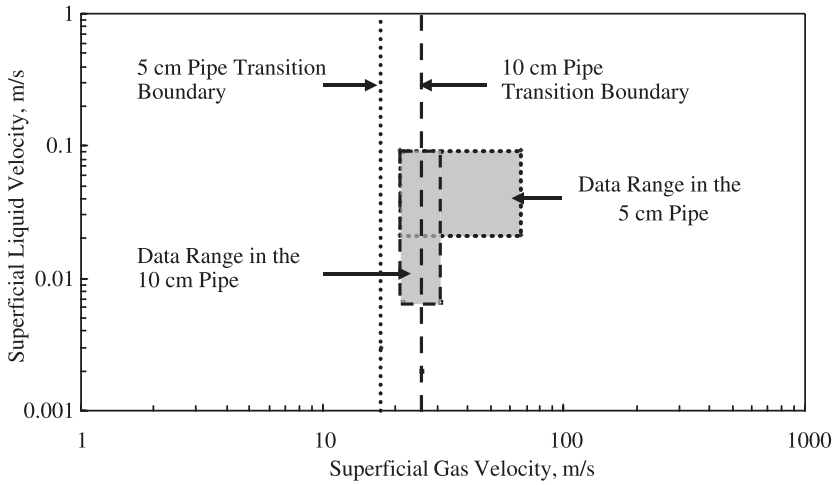

Fig. 6. Flow pattern map showing transition boundaries for two pipe sizes between the intermittent/slug and the annular dispersed flow regimes. Hatched areas show superficial velocity ranges used in the experiments.

in the 5 cm and the 10 cm pipes. It is seen that some of the data points taken from tests in the 10 cm pipe fall outside the annular dispersed flow regime.

5. Analysis and conclusions

Fig. 7 shows pressure drop data for two-phase air–water upward flow in both 5 and 10 cm pipes while in the annular dispersed regime. Similarly, Fig. 8 shows pressure drop data for two-phase air–sand upward flow in the same pipes while in the pneumatic conveying mode. The data are compared with calculations using the modified OPT model and the phenomenological pneumatic conveying model presented here. Pressure drop data obtained from two absolute pressure cells (APcells) show considerably more scatter than data obtained from one differential pressure cell (DPcell) connected between the same measurement points. This behavior is consistent throughout the collected data in this experimental program. The scatter is further magnified because of the linear scale used in the data plots instead of the commonly used logarithmic scales. Fig. 9 shows

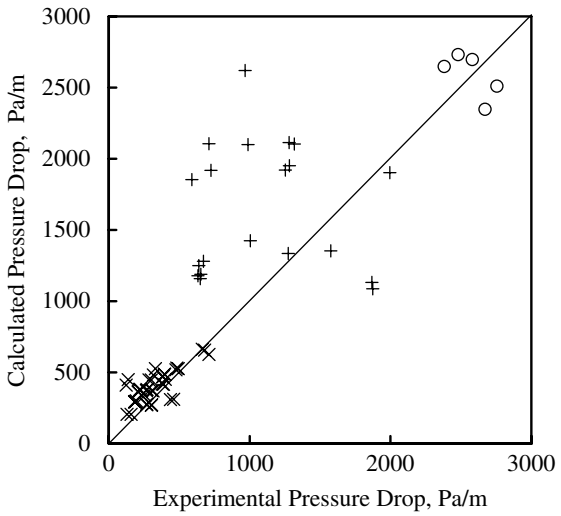

Fig. 7. Comparison between measured and calculated pressure drops in the two-phase annular dispersed gas–liquid flow experiments. $D =$ 10 cm: × with DPcell; $D =$ 5 cm: ○ with DPcell, + with two APcells.

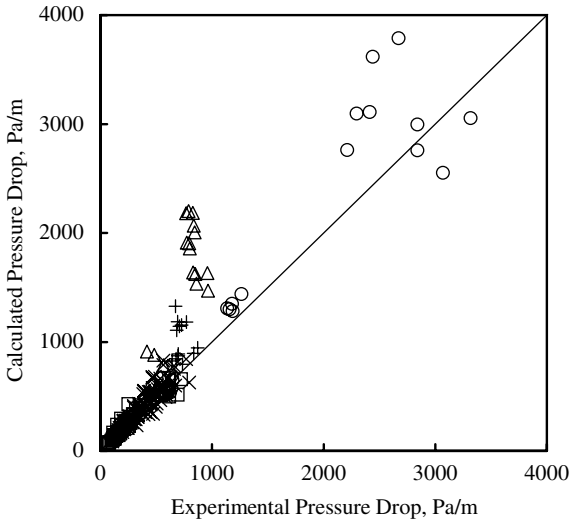

Fig. 8. Comparison between measured and calculated pressure drops in the pneumatic conveying experiments. $D = 10$ cm: □ small sand with DPcell, × medium sand with DPcell; $D = 5$ cm: ○ medium sand with DPcell, + medium sand with two APcells, △ large sand with two APcells.

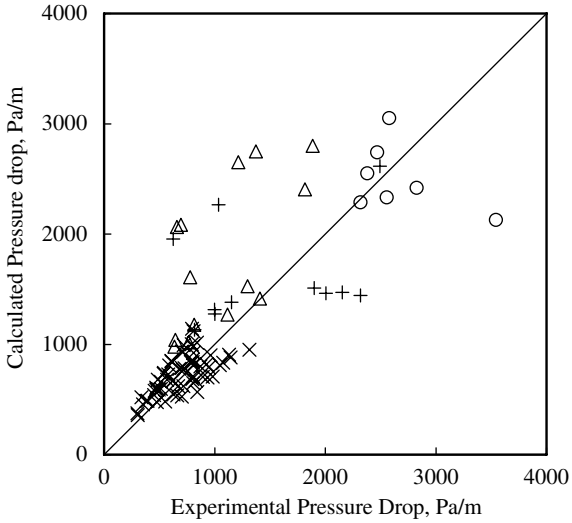

Fig. 9. Comparison between measured and calculated pressure drops in the three-phase flow experiments. $D = 10$ cm: × medium sand with DPcell; $D = 5$ cm: ○ medium sand with DPcell, + medium sand with two APcells, △ large sand with two APcells.

comparisons between measured and calculated pressure drops that resulted from the available experimental data and the integrated model calculations. Reasonably good agreement is shown for the three-phase flow model proposed here. Comparisons between the air only data and calculations were also good but are not included in the interest of brevity. The number of data points in Fig. 9 is somewhat smaller than the number in Fig. 8 because some of the data points from pneumatic conveying tests fell into the intermittent regime for gas–liquid flow. Detection and removal of these data points was straightforward because of their infrequent occurrence and the distinctive high amplitude fluctuations in the pressure drop measurement.

In summary, it is concluded that the integrated model developed here describes the behavior of the experimental data reasonably well. The calculated results suggest that direct superposition of representative gas–liquid and gas–solid flow models can be used to determine the pressure drop in annular dispersed three-phase flow systems as shown in the present application. The design approach resulting from the integrated model has

the potential of improving the sizing and selection criteria for pumps and other machinery used in this type of transport.

References

Barnea, D., Taitel, Y., 1992. Structural and interfacial stability of multiple solutions for stratified flow. Int. J. Multiphase Flow 18, 821–830.

Barnea, D., Taitel, Y., 1994. Interfacial and structural instability of separated flow. Int. J. Multiphase Flow 20 (Suppl.), 387–414.

Govier, G.W., Aziz, K., 1972. The Flow of Complex Mixtures in Pipes. Robert E. Kreiger Publishing Company Inc., Malabar, Florida (Chapter 9).

Liljegren, L.M., Bamberger, J.A., Enderlin, C.W., White, M., 1995. Pneumatic conveying of wet and dry solids through a vertical pipe. ASME Fluids Eng. Div. Publ. FED 228, 401–408.

Oliemans, R.V.A., Pots, B.F.M., Trompé, N., 1986. Modeling of annular dispersed two-phase flow in vertical pipes. Int. J. Multiphase Flow 12, 711–732.

Serghides, T.K., 1984. Estimate friction factor accurately. Chem. Eng. 91, 63–64.

Taitel, Y., Barnea, D., Dukler, A.E., 1980. Modeling flow pattern transition for steady upward gas–liquid flow in vertical tubes. AIChE J. 26, 345–354.